Theoretical Modeling of Shielding for Plasma Flow and Electron Beam Heating

V.A. Popov[1,2,a)], A.S. Arakcheev[1,2,3], A.V. Burdakov[1,3], A.A. Kasatov[1], A.A. Vasilyev[1] and L.N. Vyacheslavov[1,2]

[1]*Budker Institute of Nuclear Physics SB RAS, 11 akademika Lavrentieva , Novosibirsk 630090, Russia*
[2]*Novosibirsk State University, 2 Pirogova Str., Novosibirsk 630090, Russia*
[3]*Novosibirsk State Technical University, 20 K. Marksa prospect, Novosibirsk 630090, Russia*

[a)]Corresponding author: v.a.popov94@gmail.com

Abstract. Electron beam appears to be a good instrument for the simulation of heat loads because of low pressure to material and large depth of shielding layer, allowing for the application of higher loads. This work is focused on theoretical and numerical modeling of heating tungsten by plasma flow and electron beam heating to clarify differences in the heating process. The time necessary for vapor shielding development is found for both of them. Essential time differences between electron beams with various energies were found. It was explained by significant cooling by evaporation at one of the heating stages. The surface temperature is almost stabilized and the maximal temperature location shifts under the surface at this stage.

INTRODUCTION

The next generation of experimental fusion reactors is expected to have intensive flows of plasma particles and radiation on the first wall and divertor plates [1]. The loads on materials lead to a number of erosive processes and degradation mechanisms: sputtering, melting, boiling, splashing, etc. The rate of erosion depends on the dominant mechanism. With intense heat fluxes, the rate of erosion can be extremely high. Electron beam facilities, lasers and quasi-stationary plasma accelerators can model such heat loads for refinement of surface parameters required for understanding of the thresholds between dominating mechanisms. The heating is considered to be limited by the vapor shielding. So, especially an electron beam seems to be a good simulation instrument because of low pressure to material and large depth of shielding layer, allowing one to simulate higher heating loads. This work is focused on theoretical and numerical modeling of material heating by plasma flow and electron beam heating to clarify differences in the heating process. All calculations were made for tungsten as a preferable material for the divertor.

MODEL OF HEATING

For calculation of the spatial and temporal distribution of temperature during pulsed heat loads, the following effects have been taken into account: vapor shielding, cooling by evaporation, volumetric heating, and temperature dependence of material properties. The significant influence of the effects was demonstrated in [2, 3]. The motion of liquid was not taken into account.

Model of Energy Release

The vapor shielding at different models of ion stopping by the material was studied in [4]. Similar results were demonstrated for models in a wide range of parameters. So, the energy release is considered to be volumetric and constant per unit mass. The energy released in the vapor is proportional to the mass of evaporated layer. The energy does not reach the surface because of low thermal conductivity in the vapor and light emission to all directions, not only to the heated surface. In this way the surface is shielded by the vapor. The stopping ranges for electrons

in different materials are well known and tables were published by ICRU [5]. The plasma ions stopping range was assumed to be 0.1 μm according to the results of work [4].

Model of Thermal Propagation

Temperature in liquid and solid materials diffuses according to the heat conduction equation

$$C(T)\frac{\partial T}{\partial t} = \frac{\partial}{\partial x}\chi(T)\frac{\partial T}{\partial x} + N(x,t), \tag{1}$$

where T is the temperature; x is the distance from the initial surface; t is the time; C is the thermal capacity; χ is the thermal conductivity; $N(x,t)$ spatial and temporal distribution of power density. The data on the thermal conductivity and capacity temperature dependencies are taken from [6, 7, 8]. The discontinued parameters of the material at the melting point were smoothed. The specific melting heat was added to the capacity as a gaussian function with a standard deviation of 30 °C.

There are two boundary conditions at the surface: moving of the surface with the rate of evaporation into vacuum [9] and energy losses from the surface via evaporation and radiation,

$$\dot{x}_{surf}(t) = \frac{P(T(x_{surf}(t),t))}{\rho}\sqrt{\frac{M}{2\pi mRT(x_{surf}(t),t)}} \tag{2}$$

$$L(T(x_{surf},t))\frac{dx_{surf}}{dt} + \alpha(T)\sigma T(x_{surf},t)^4 = \chi(T(x_{surf},t))\frac{\partial T(x_{surf},t)}{\partial x}, \tag{3}$$

where x_{surf} is the thickness of evaporated layer; σ is the Boltzmann constant; α is the emissivity; $L(T)$ is the specific heat of evaporation [10]; P is the pressure of saturated vapor [6]; M is the molecular mass; R is the gas constant; ρ is the density of material. Note that the radiation power is less than the cooling power by evaporation at temperatures of above 5000 °C.

Finite difference implicit method with linearizing with tridiagonal matrix algorithm were used to solve equations numerically.

RESULTS

The discussed model was applied to simulations of pulsed heating of tungsten with durations of hundreds of microseconds and power densities of tens of GWm^{-2} . The parameters are typical to the PMI (plasma material interaction) electron beam facility at Budker Institute[11]. The election energy at the facility is 100 keV.

Vapor Shielding

The vapor shielding is supposed to limit the surface temperature at lower value for the heating by plasma ions than for the electron beam heating. It is a result of the wider stopping range of electrons in a material than that of ions. So, the thickness of the layer necessary to shield the surface in the case of electron beam heating is assumed to be significantly bigger than that in heating by a plasma flow. Consequently, the heating duration necessary to shield the surface has to be significantly different for heating by an electron beam and a plasma flow. The achievement of 100 % shielding may be a slow process. So, it cannot characterize the typical duration of the vapor shielding development. Thus, a time threshold for the shielding development was chosen as the time from the heating to the moment when 30 % of heating power is shielded by the vapor layer. The results of the calculation are shown in Fig. 1(a).

The ratio of the stopping ranges of an ion and a 50 keV electron is about 50, while the ratio for 100 keV and 50 keV electrons is about 3. However, Fig. 1(a) demonstrates that the ratios of the calculated durations of the shielding developments for these sorts of particles do not differ so dramatically. We examined the time dependence of surface temperature in heating by 100 keV electrons with 20 GWm^{-2} heating power during 300 μs shown at Fig. 2 to explain the disagreement in Fig. 1(b). The comparison of the heating without vapor shielding and with it demonstrated that the temperature growth stops before the vapor shielding becomes significant. The surface temperature growth ends when the cooling by evaporation increases to values comparable with the incident power. At the first stage, there is no influence of the surface cooling and vapor shielding on the heating because of the low temperature and high incident

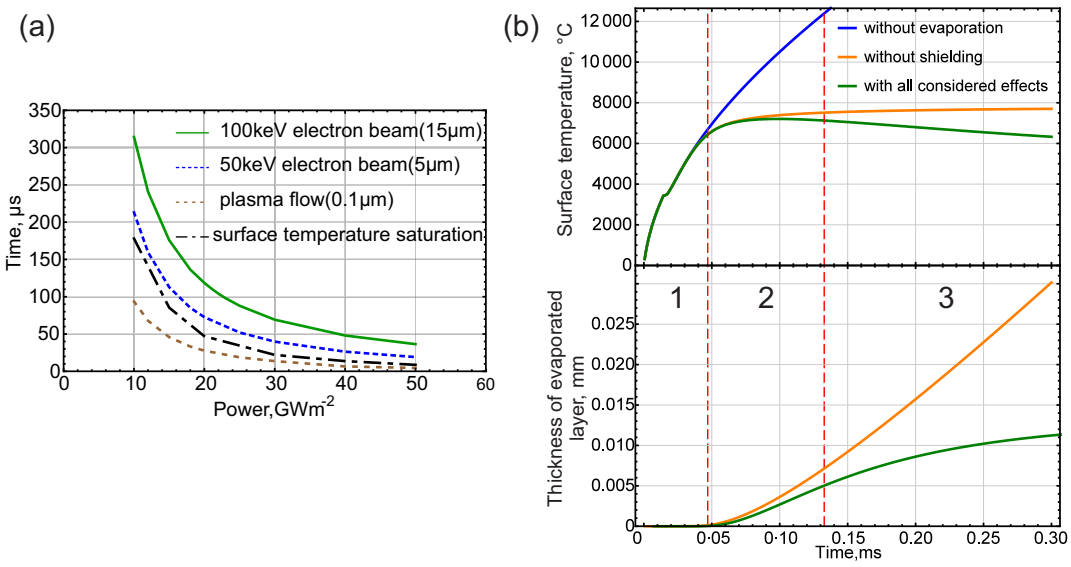

FIGURE 1. (a) Time required for evaporation of 30 % of shielding layer in the cases of 50 keV, 100 keV electron beams and plasma flow heating. Lengths in brackets is considered stopping ranges. Dash-doted curve is time required for heating surface to reach temperature at which the cooling by evaporation becomes 30 % of incident power in flow. (b) Surface temperature time dependence for 3 different simulations: evaporation switched off, vapor shielding switched off and both taken into account. In addition, the vertical dashed lines show the moments at which the evaporation takes away 30 % of the incident power and at which the evaporated layer starts shielding 30 %. Parameters of simulation: 15 μm stopping range (100 keV electron beam), 20 GWm^{-2} heating power with heating duration of 300 μs.

heating power. In the figure the stage is marked with 1. Without evaporation the temperature grows terrifically. So, at some moment the evaporation starts being important. The moment at which the cooling by evaporation takes away 30 % of the energy of the incident flows is shown with the dash-dotted curve in Fig. 1(a) and the first vertical dashed line in Fig. 1(b). We chose this condition to unify the criterium for the times plotted in Fig. 1(a). Roughly after that moment, the temperature grows slowly because a significant part is taken away by the evaporation. The evaporation rate increases to a constant value because it is roughly proportional to the cooling power. This period is marked with 2. Without vapor shielding, the evaporated layer increases proportionally to the time of heating, and the temperature also grows up to a constant. At some moment, the thickness of the evaporated layer becomes comparable with the stopping range. This moment is shown with the solid curve in Fig. 1(a) (a 100 keV electron beam was used for the example) and the second dashed vertical line in Fig. 1(b). After that moment, the temperature decreases because the heating power is reduced following the vapor shielding development. This period is marked with 3.

Superheated Liquid

The presence of stage 2, at which the heating and cooling are mostly balanced and the vapor shielding is not essential, leads to some new effects. One of important effects is that the maximum temperature is shifted to under the surface. In this mode, the liquid is under a pressure lower than the pressure of saturated vapor. For estimation of the temperature difference between the surface and the maximum we can make simplifications for equation 1. At first we suppose that the evaporation is static (depending only on $x - x_{surf}(t)$) and rate of evaporation is small ($\dot{x}_{surf} \ll \chi/C\lambda$). In this case we can neglect time dependence in the co-moving coordinate system. At this layer $\nabla T/T \gg \nabla\chi/\chi$, so we can neglect it too. In this way, the desired temperature difference can be found as follows:

$$\delta T = \frac{P_{surf}\lambda\beta^2}{2\chi}, \tag{4}$$

where P_{surf} is the power that achieve the surface through the vapor layer and β is the ratio of the power lost via evaporation to P_{surf}. This estimation gives an additional pressure of up to 20 % of the pressure at the surface. So,

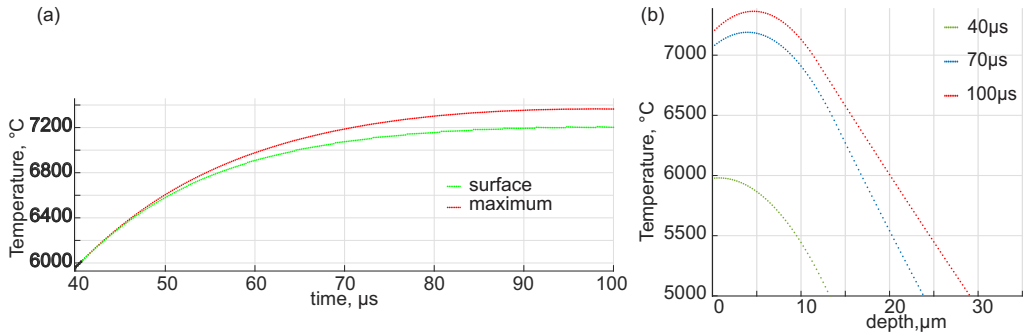

FIGURE 2. In these figures the temperature is shown for heating by a 100 keV electron beam (15 μm) with a 20 GWm^{-2} heating power during 100 μs (a) time dependence for surface and maximum temperature. (b) distribution of temperature in the liquid near the surface for 3 different moments: 40 μs (stage 1) and 70 μs and 100 μs (stage 2).

the liquid under the surface is superheated and the melt may boil. The boiling may cause splashing with ejection of droplets [12].

CONCLUSIONS

The duration of heating necessary for vapor shielding development was calculated for electron beam and plasma flow heating. Essential differences in the durations with electron beams with various energies were found. The significant difference is caused by cooling by evaporation before the vapor shielding development. The temperature of the surface is almost stabilized at this stage. Also the location of the maximum temperature shifts under the surface and the layer of the liquid becomes superheated. The latter may cause boiling of the melt.

ACKNOWLEDGMENTS

This work was supported by Russian Science Foundation (project N 14-50-00080).

REFERENCES

[1] G. Janeschitz, K. Borrass, G. Federici, Y. Igitkhanov, A. Kukushkin, H.D. Pacher, G.W. Pacher, M. Sugihara, J. Nucl. Mater. 220-222(1995), pp. 73-88.
[2] A.V. Burdakov, M.N. Chagin, V.V. Filippov, V.S. Koidan, K.I. Mekler, P.I. Melnikov, V.V. Postupaev, A.F. Rovenskikh, M.A. Shcheglov, K.V. Tsigutkin, H. Wuerz, 1996. J. Nucl. Mater. 233-237, pp. 697-700.
[3] I. Poznyak, N. Arkhipov, S. Karelov, V. Safronov, D. Toporkov, in Proceedings of the 39th International Conference on Plasma Physics and Controlled Fusion, Zvenigorod, 0610 February (2012).
[4] D.I. Skovorodin, A.A. Pshenov, A.S. Arakcheev, E.A. Eksaeva, E.D. Marenkov, and S.I. Krasheninnikov, Phys. Plasmas **23**, 022501 (2016)
[5] ICRU, 1984. ICRU Report 37, Stopping Powers for Electrons and Positrons.
[6] J.W. Davis, P.D. Smith, 1994. Iter Material Properties Handbook.
[7] M. W. Chase, Jr.,1998, Nist-Janaf Thermochemical Tables, Fourth Edition, Monograph 9
[8] G., Pottlacher, 1999. J. Non-Cryst. Solids. 250-252(1), pp. 177-181
[9] S. Shiller U. Heisig, S. Panzer, Electron beam technology(John Wiley & Sons, Australia,1982)
[10] K.M. Watson, Ind. Eng. Chem., **1943**, 35 (4), pp. 398-406
[11] L.N.Vyacheslavov, et al., "Novel electron beam based test facility for observation of dynamics of tungsten erosion under intense ELM-like heat loads", AIP Conf. Proc. (these proceedings)
[12] A.A.Kasatov, et al., "Observation of dust particles ejected from tungsten surface under impact of intense transient heat load", AIP Conf. Proc. (these proceedings)